Final Report

Modeling Southern California with Faulted Lithosphere

Eugene Humphreys, University of Oregon

Two major projects have been addressed during the final year of SCEC2, both nearing submission and both involving recent Ph.D. graduate Noah Fay. One project involved the modeling of forces acting on the Sierra Nevada block, and the other involving modeling of faulted lithosphere.

(A) Forces acting on the Sierra Nevada Block.
Using 2-D finite element modeling, we estimate the loads acting on the Sierra Nevada block to predict the stresses within the block. We find the optimal set of loads (bottom right frame of Fig. 1) by minimizing the misfit between the observed (upper left frame) and modeled (upper right frame) stress. By using the stresses resulting from gradients in the gravitational potential energy (lower left frame), we obtain absolute stress estimates for the lithosphere. The two most important results are:
(1) San Andreas Fault strength (stress level) depends strongly on location, varying from 2.6 TN/m to 0.3 TN/m (bottom center and right frames). With reasonable strength

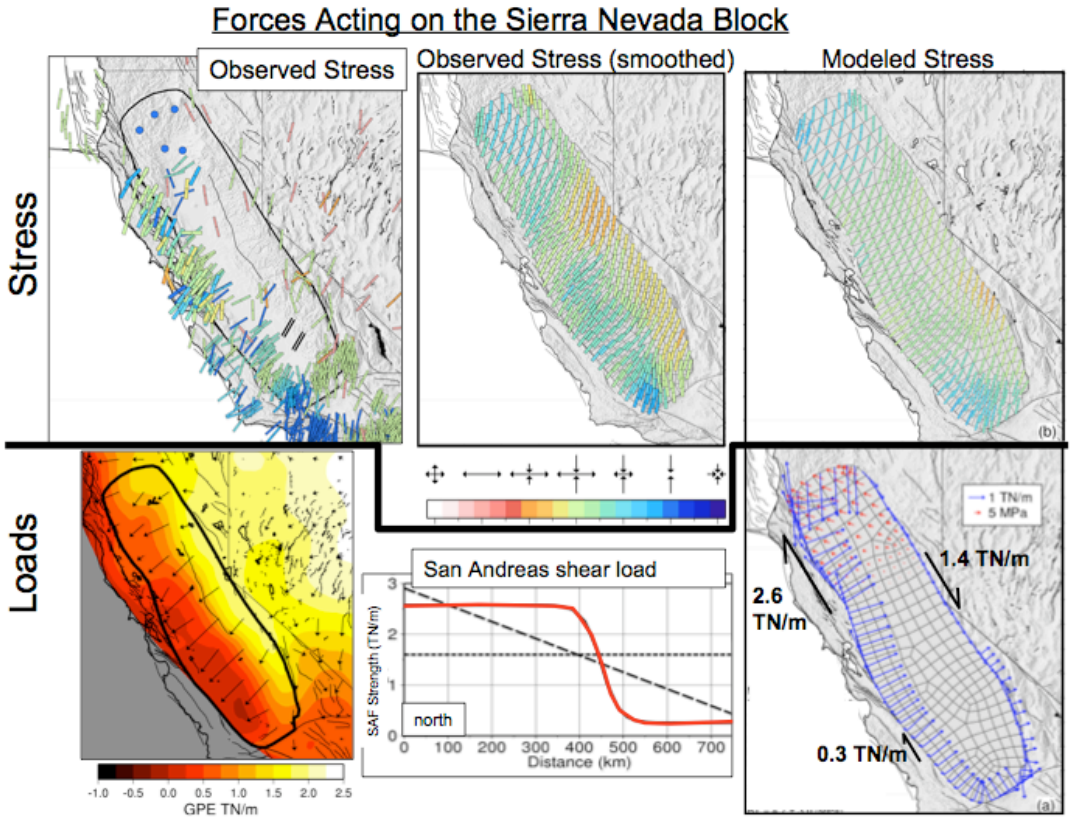

Figure 1. Stresses and modeled loads acting on the Sierra Nevada block. In top row of frames, bars show maximum horizontal compression orientation, and color indicated tectonic style. Bottom left frame shows gravitational potential energy, bottom center frame shows modeled San Andreas shear stress integrated through the lithosphere, and bottom right frame shows modeled side and basal loads (with the shear tractions emphasized for clarity).

profiles, these values give mid-crustal stress levels of 25-60 MPa and 3-6 MPa, respectively. The weakest San Andreas is largely the creeping section. For the stronger seismogenic section, the stresses yield an effective friction coefficient of 0.05-0.1 (low strength), but they are many times the ~3 MPa stress drop of a typical earthquake. (2) The load applied on the Sierra Nevada block by Pacific plate coupling (i.e., those discussed in (1)) are resisted by shear tractions on the block's east side (an average of 1.4 TN/m) and by compressive stresses on the block's northern end. This latter load represents the compression between the Sierra Nevada block ant the Coast Ranges of the Pacific Northwest (the accreted Siletzia ocean lithosphere). Such stress interaction at a distance has important effects on southern California.

This work is now completed and we are in the process of writing it up for publication.

(B) Modeling of faulted lithosphere; lithospheric stress near the San Andreas Fault. The distribution of lithospheric strength and the corresponding distribution of deformation mechanisms currently are not well known and are actively debated (e.g., Jackson, 2002; Burov and Watts, 2006). These are important to un derstand because they relate to the means by which the crust and faults are loaded and the physical parameters controlling earthquake rupture. We constrain the vertical distribution of stress (in particular in the crust) near the San Andreas Fault through elastic-plastic-viscous thermo-mechanical finite element modeling of stress and strain rate. Deformation mechanisms are elastic for the upper crust, plastic for faults, and viscous at sub-seismogenic depths; all deformation domains are determined dynamically, as illustrated in an example shown in Fig. 2. The model is 2.5 dimensional, i.e., perpendicular to the strike of the fault with motion into the page, and symmetrical about the vertical fault (the right-most thin zone in Fig. 2). For a given coefficient of friction (or depth-averaged fault strength, DAFS in Fig. 2), and lower crust and upper mantle viscosity parameters (Ac and Am in the figure) we determine the steady- state distribution of stress, temperature, strain rate and deformation mechanism. Through a grid-search of model parameters we determine which parameters satisfy available observations of faulting depth (e.g., Scholz, 1988), crustal strain rate (e.g., Zoback et al., 1992) stress magnitudes in the crust (e.g., Townend and Zoback, 2004) and integrated lithospheric stress (Humphreys and Coblentz, 2007). This set of constraints limits successful models to be similar to that shown in Fig. 2. The depth-average fault strength is constrained to be ~20-50 MPa, and effective lower crust viscosity is bracketed between ~5e19 and 5e20 Pa-s. We see in this figure that for this model deformation plastic in the fault, elasto-plastic (essentially elastic; see deformation rate frame) in the upper crust, and visco-elastic in the lower crust and upper mantle. Stress in the fault and directly below is shown in the top center frame, where a rather classic "Christmas tree" strength profile is seen. Fault stress in the mid-crust attains values of ~70 MPa. Away from the fault, mid-crustal stresses attain values as great as 100 MPa. If frictional heating is allowed to occur on the fault, heat flow is unreasonably great (black line in Heat Flow frame of Fig. 2). Instead, we infer slip is associated with a dynamic weakening of the fault, yielding acceptable heat flow values (red line in this frame). Deformation in this model broadens with depth, but because of shear heating it widens relatively slowly with depth. At 70 km depth deformation is about 70 km wide.

This work is nearly completed and we are beginning to write it up for publication.

Figure 2. Example dynamic model of a strike-slip fault. The rheologic flow parameters Ac & Am and depth-averaged fault strength (DAFS) define the model. In this model, integrated strength of the mantle and the crust are nearly equal (values in top center frame, given in TN/m), and high degrees of lower crustal decoupling occur. Other successful models have most strength in the crust, with a stronger lower crust.